

PHYSICAL REVIEW B

CONDENSED MATTER AND MATERIALS PHYSICS

THIRD SERIES, VOLUME 60, NUMBER 22

1 DECEMBER 1999-II

RAPID COMMUNICATIONS

Rapid Communications are intended for the accelerated publication of important new results and are therefore given priority treatment both in the editorial office and in production. A Rapid Communication in Physical Review B may be no longer than four printed pages and must be accompanied by an abstract. Page proofs are sent to authors.

Raman-active modes of α -GeSe₂ and α -GeS₂: A first-principles study

Koblar Jackson, Arlin Briley, and Shau Grossman

Department of Physics, Central Michigan University, Mt. Pleasant, Michigan 48859

Dirk V. Porezag and Mark R. Pederson

Center for Materials Simulation, U.S. Naval Research Laboratory, Washington D.C. 20375

(Received 26 August 1999)

We have used a recently developed computational technique based on density-functional theory to study the Raman-active modes of amorphous GeSe₂ and GeS₂. Vibrational modes and the associated Raman activities for three cluster building blocks of the glasses are calculated directly from first principles. The positions of the calculated symmetric-stretch modes in the cluster models are in excellent agreement with sharp features in the observed spectra. Moreover, simulated spectra based on the cluster results are in good agreement with experiment, accounting for all the observed features in the bond-stretch region of the spectra. The cluster results suggest a new interpretation for the 250 cm⁻¹ mode appearing in the spectra of Ge-rich samples in the Ge_xS_{1-x} family. [S0163-1829(99)51846-8]

Raman spectroscopy has been an important tool for investigating the properties of chalcogenide glasses for over two decades.¹⁻⁴ Applications have ranged from early investigations of short-range order in the glasses^{3,5,6} to very recent probes of network rigidity.⁷⁻⁹ The Raman spectra of glasses such as GeS₂ and GeSe₂ are interesting because they contain sharp, molecularlike features that can be associated with local structural elements of the materials. The molecular nature of the spectra has motivated calculations based on atomic clusters to interpret the spectral features.^{1,2} These calculations used empirical force fields to compute vibrational modes¹⁰ and in some cases bond polarization models to compute Raman intensities.¹¹⁻¹³ Such calculations gave a useful qualitative understanding of the spectra but were limited by the empirical nature of the models in the amount of detail they could provide. Higher level calculations have been applied to bulk α -GeSe₂^{14,15} and to liquid GeSe₂,¹⁶ but these calculations were not aimed at interpreting the Raman spectrum.

In this paper we use a first-principles method based on the density-functional theory (DFT) to study the Raman spectra of GeSe₂ and GeS₂. We use standard DFT techniques to obtain the vibrational normal modes of cluster models and

then a DFT-based method¹⁷ to compute the associated Raman activities. We show that the main features of the observed spectra are reproduced in excellent agreement with experiment and that the overall spectra can be simulated very well using only the results of cluster calculations on three simple structures. Finally, we use the results of our calculations to suggest a new interpretation for the 250 cm⁻¹ mode observed in Ge-rich compositions of Ge_xS_{1-x}.⁴

The calculations described here are based on the density-functional theory in the local-density approximation (LDA).¹⁸⁻²⁰ We use a Gaussian-orbital-based formulation of the theory, with a robust numerical integration scheme²¹ that gives highly accurate total energies and atomic forces.²² The cores of the heavy atoms are represented by norm-conserving pseudopotentials,²⁴ while the H atoms are included in an all-electron framework.²³

To study the Raman-active modes of GeS₂ and GeSe₂, we use finite clusters of atoms containing structural units expected to be important in the glasses. Dangling bonds on the cluster surfaces are terminated by H atoms, to better model the chemical environment of the glasses. The cluster geometries are optimized using a conjugate-gradient algorithm, and the vibrational normal-mode frequencies and eigenvec-

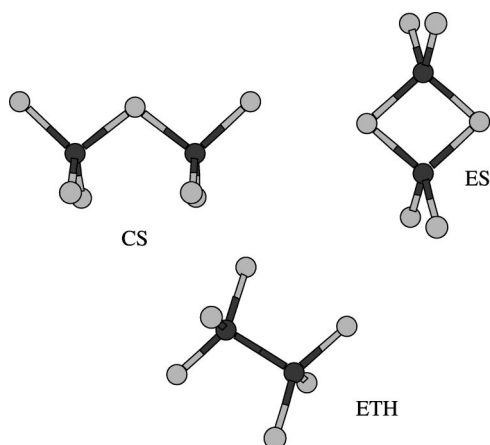


FIG. 1. The corner-sharing (CS), edge-sharing (ES), and ethane-like (ETH) cluster models studied here.

tors are computed using standard techniques. The large mass difference between H and the heavy atoms prevents H-atom motion from mixing strongly in the Ge-X vibrational modes. The bulk of the H-atom modes lie well outside the spectral region of interest for GeS_2 or GeSe_2 . Any H-atom modes that do fall in this region are removed from the analysis.

The key feature of this work is our ability to compute Raman activities for each of the vibrational modes directly within the LDA.¹⁷ The Raman-scattering activity, I^{Ram} , associated with a given vibrational mode is related to the change in the electrical polarizability of the material due to the normal-mode displacements of the atoms.²⁵ The essential ingredients are the gradients of the polarizability with respect to the nuclear coordinates:

$$\frac{\partial \alpha_{ij}}{\partial R_k} = - \frac{\partial^3 E}{\partial G_i \partial G_j \partial R_k} = \frac{\partial^2 F_k}{\partial G_i \partial G_j}, \quad (1)$$

where E is the cluster total energy, G_i is the i th component of an external electric field, and F_k is the calculated force on the k th atomic coordinate. We calculate the field derivatives by finite differences using forces from independent self-consistent calculations with small applied electric fields.²⁶ We have found that field strengths on the order of 0.005 a.u. yield converged results for the derivatives.¹⁷

The basic structural building blocks for GeS_2 and GeSe_2 are Ge-centered tetrahedra, GeX_4 . These can be connected in two simple ways in the glasses, by sharing a single corner or an edge. The corner-sharing (CS) and edge-sharing (ES) structures are illustrated in Fig. 1. (Another possibility is to share three X atoms to form face-sharing tetrahedra, but our calculations²⁷ suggest such a structure is energetically unfavorable and we do not consider it further here.) The third cluster shown in Fig. 1 is an ethanelike (ETH) structure, the simple structure exhibiting Ge-Ge bonds. Clear experimental evidence for broken chemical order exists for both GeSe_2 and GeS_2 .^{4,28}

We list the frequencies and calculated Raman activities for the main Raman-active cluster modes in Table I and compare them with the positions of peaks in the observed spectra.³ The agreement between the calculated and observed frequencies shown in Table I is striking. Both ES modes are within 1 cm^{-1} of the observed A_{1c} peaks and the selenide

TABLE I. A comparison of observed peak positions in GeS_2 and GeSe_2 with calculated Raman-active modes for the clusters shown in Fig. 1. The A_1 and A_{1c} peaks are labeled A and C for convenience. Also given are the calculated absolute Raman intensities (I^{Ram}) of the different cluster modes and the clusters in which they appear.

mode	Ge_2		I^{Ram} ($\text{\AA}^4/\text{amu}$)	cluster model
	ω^{Exp} (cm^{-1})	ω^{Th} (cm^{-1})		
	250	254	39.1	ETH
A	343	335	77.5	CS
C	374	373	79.3	ES
		366	45.1	ETH
	437	436	6.7	ES
	179	179	49.2	ETH
A	202	195	47.9	CS
C	218	219	40.5	ES
		288	3.9	ETH
	310	319	7.7	ES

ethanelike mode is in perfect agreement with the position of an observed peak that is associated with Ge-Ge bonds.²⁸ Both CS modes are slightly softer than the observed A_1 peaks. The differences are small and may simply reflect the inherent limitation of the LDA in calculating frequencies. The differences may also have a structural origin. Recent experiments have shown that the A_1 peaks shift to higher frequency with Ge content as the glasses go through the rigidity transition.⁷ Below the transition, at around $x=0.23$, the measured A_1 frequency is 195 cm^{-1} for $\text{Ge}_x\text{Se}_{1-x}$ and 341 cm^{-1} for $\text{Ge}_x\text{S}_{1-x}$. These frequencies are closer to the calculated values shown in Table I. The CS clusters apparently model the A_1 modes in the floppy regime better than in the rigid regime. No systematic shift of the A_{1c} modes in these systems was mentioned in Ref. 7.

In Fig. 2 we present simulated spectra for GeS_2 and GeSe_2 , derived from the cluster results. For comparison we show the corresponding observed spectra³ in the insets. The simulated spectra represent Gaussian-broadened densities of states of the cluster modes, weighted by the calculated Raman intensities. To keep the simulated spectra as unbiased as possible, the width assumed for each cluster mode is set equal to the width of the nearest feature in the observed spectra as assigned in the analysis of Sugai.³ We have shifted the frequencies of the two CS symmetric stretch modes to bring them into agreement with the observed A_1 peaks shown in Table I. This makes the ethanelike mode in GeSe_2 a more pronounced shoulder and has no effect on other parts of the simulated spectrum.

Creating the simulated spectra also requires specifying the relative concentrations of the CS, ES and ETH structures. These are deduced from experiment by assuming that the total integrated intensities for the A_1 , A_{1c} , and ethanelike peaks in the observed spectra are proportional to the product of the concentration of the corresponding CS, ES, and ETH structural features and the calculated absolute intensities of the cluster modes:

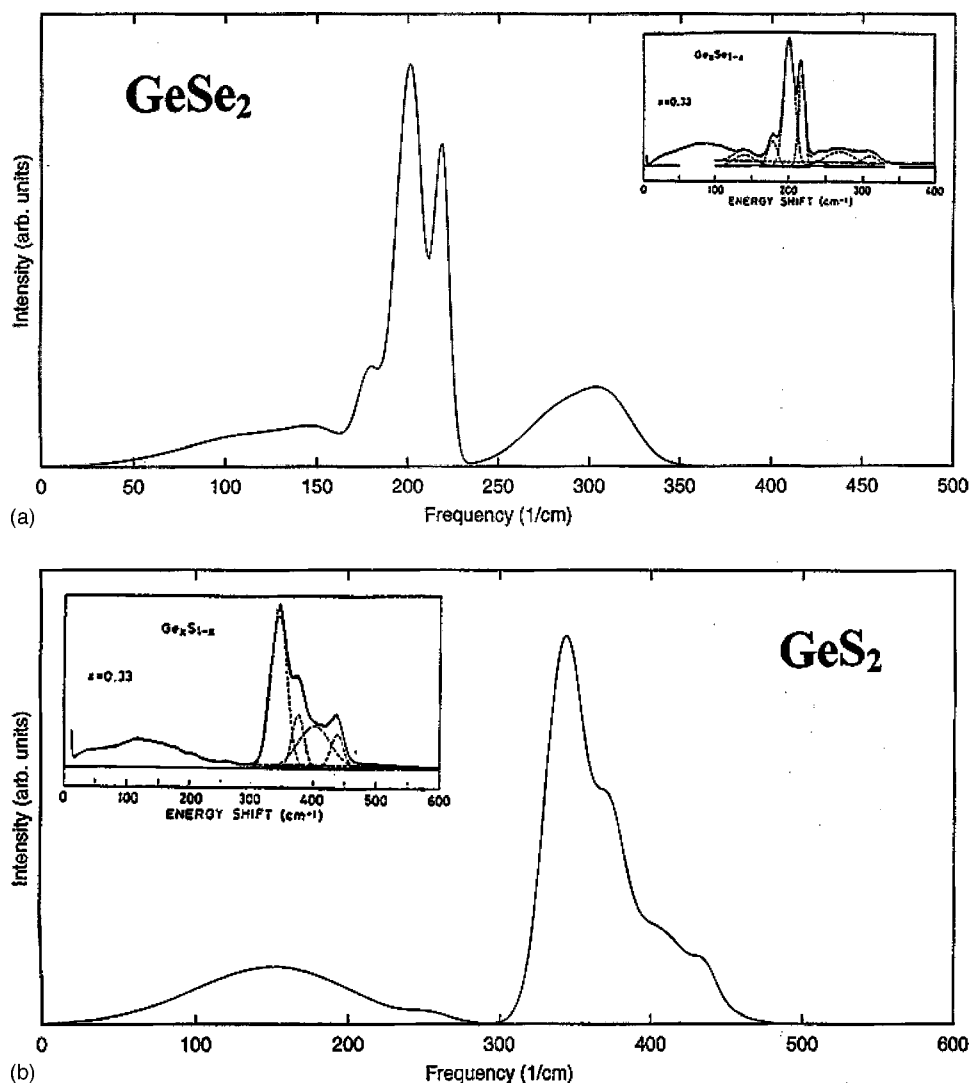


FIG. 2. Simulated and observed Raman spectra for GeSe₂ and GeS₂. The observed spectra shown in the insets are taken from Ref. 3. The simulated spectra were obtained from the cluster calculations as described in the text.

$$I_i^{exp} \propto C_i \cdot I_i^{th}, \quad (2)$$

where I_i^{exp} is the observed intensity, I_i^{th} is the calculated absolute intensity of the cluster mode and C_i is the concentration. By also assuming that the concentrations sum to one, we arrive at concentrations of 0.77, 0.22, and 0.01 for the CS, ES, and ETH structures for GeS₂ and 0.58, 0.33, and 0.09 for GeSe₂.

The simulated GeS₂ spectrum shown in Fig. 2 is in excellent agreement with the measured spectrum, reproducing all the observed features in the bond-stretching region at the proper positions. The calculations also produce modes in the bond-bending region below 250 cm⁻¹, but since the experimental spectrum in this region is bandlike, we do not expect to reproduce it in the cluster calculations. The broad feature at around 400 cm⁻¹ contains contributions from both the CS and ES clusters, but the peak at about 436 cm⁻¹ is due entirely to the highest mode in the ES cluster. Previous empirical force field calculations assigned this mode to S-S modes,¹² but these lie higher, at frequencies near 480 cm⁻¹, in the spectra for S-rich compositions reported by Sugai.³ The association of the 436 cm⁻¹ mode with the ES structure implies that the intensity of this feature should track that of

the A_{1c} peak at 373 cm⁻¹. A visual inspection of the spectra made as a function of Ge content in Ref. 3 suggests that such a relationship exists.

For GeSe₂, the simulated and observed spectra agree very well in the A₁ region (170–230 cm⁻¹) and at frequencies above 280 cm⁻¹, but differ in between. The experimental spectrum contains broad peaks centered around 240 and 270 cm⁻¹ that are missing in the calculated spectrum. These features appear to be related to Se-Se bonds, since they become much more prominent for Se-rich compositions.³ We have studied²⁷ simple models containing Se-Se bonds and find the Se-Se stretch frequencies to fall near 270 cm⁻¹. Furthermore, we find no Ge-Se modes in any of our cluster calculations between 220 and 276 cm⁻¹. We therefore attribute the difference between the simulated and observed spectra to the absence of Se-Se related features contributing the former. The highest feature in the simulated spectrum, lying at 319 cm⁻¹, comes from the ES structure. We associate this with the small experimental peak observed at 310 cm⁻¹ by Sugai.³

There is an interesting difference between the spectra for GeSe₂ and GeS₂ in the region below the A₁ peak. There is a prominent peak at 179 cm⁻¹ for GeSe₂, but only a very weak feature around 250 cm⁻¹ for GeS₂. Both these features

are known^{4,28} to depend sensitively on the Ge content of the sample, appearing only in Ge-rich samples. The 179 cm^{-1} peak has been assigned to ethanelike units.^{10,28} This assignment is supported by our calculations which find a Raman-active mode for the ETH cluster at 179 cm^{-1} (see Table I). Similarly, our calculations find a Raman-active mode at 254 cm^{-1} for the ETH cluster in the sulfide case, and by analogy to the selenide case, we assign it to the observed 250 cm^{-1} mode in GeS_2 . A similar assignment was previously made by Lucovsky,¹⁰ however this mode has also been assigned⁴ to a Ge-rich rock-salt-like structure (the *C* sites in Ref. 4) similar to that found in *c*-GeS. That assignment was based on two arguments. First, the peak falls very near the known 240 cm^{-1} Raman line of *c*-GeS.²⁹ In addition, the weakness of the 250 cm^{-1} peak appears to be inconsistent with the Mössbauer site intensity data⁴ that suggest the concentration of ethanelike or *B* sites in GeS_2 is greater than in GeSe_2 . The Raman signature for the *B* sites was assumed to be obscured by the A_1 or A_{1c} peaks in Ref. 4.

If the 250 cm^{-1} mode is to be assigned to the *B* sites, as our calculations suggest, why is it so weak in the observed spectrum? Our calculations are consistent with a weak 250 cm^{-1} mode in two ways. First, as shown in Table I, the Raman intensity of the sulfide ETH cluster is split between two modes, one at 254 cm^{-1} and the other at 366 cm^{-1} , directly between the A_1 and A_{1c} peaks. The 254 cm^{-1} mode that we associate with the observed feature has only 1/2 the intensity of the corresponding CS mode, while in the selenide case, the ETH mode has a slightly larger intensity than the CS mode. Thus, for equal relative concentrations of ETH units to CS units in the glasses, the 250 cm^{-1} mode in GeS_2 would have only 1/2 the intensity compared to the A_1 peak as the 179 cm^{-1} peak in GeSe_2 . Second, the calculated binding energies for the various clusters are consistent with a smaller concentration of ETH units in GeS_2 than GeSe_2 . This would also make the 250 cm^{-1} mode weaker compared to the 179 cm^{-1} selenide mode. In the sulfide case, the ETH cluster is 0.16 eV per bond less stable than the CS and ES clusters,³⁰ while in the selenide case, the ETH cluster is only 0.08 eV per bond less stable. Formation of the ETH units should therefore be more favorable in GeSe_2 than in GeS_2 . Further, the lack of S-S related features near 480 cm^{-1} in the observed spectrum also suggests a low concentration of *B* sites. Such features should be expected on bond-counting grounds given a significant concentration of Ge-Ge bonds. Analogous Se-Se features are seen in the GeSe_2 spectrum, as noted above.

Regarding the Mössbauer site intensity data, which give a *B* site intensity of about 0.3 for GeS_2 and only about 0.2 for GeSe_2 , we note the discussion in Ref. 4 that the site intensities are not directly proportional to concentrations. Site energetics for the Mössbauer tracer Sn atoms must also be taken into account. It is possible that site intensity data overestimate the population of the *B* sites in GeS_2 .

Given the different interpretations of the 250 cm^{-1} mode, additional work may be needed to settle the issue. Experimentally, a careful line-shape analysis of the Raman spectra could be done to search for the predicted 366 cm^{-1} ETH mode for *x* near 1/3 in $\text{Ge}_x\text{S}_{1-x}$. The intensity of this mode should grow in proportion to that of the 254 cm^{-1} mode. On the theory side, it would be interesting to construct models of the *C* sites, in order to calculate their Raman signatures. This would facilitate a more detailed interpretation of the Raman spectra for samples with $x > 1/3$. A *C*-site Raman feature near 240 cm^{-1} would be difficult to resolve from *B*-site features at 250 cm^{-1} .

In this paper we have used a first-principles method to investigate the Raman-active modes of the chalcogenide glasses GeS_2 and GeSe_2 . The method is used to calculate both the frequencies and the corresponding Raman activities of the vibrational modes for cluster models of the glass. The calculated frequencies of the symmetric-stretch modes of these clusters are in excellent agreement with the positions of the sharp peaks in the observed spectra. In addition, the calculated Raman intensities allow a detailed comparison between theory and experiment, resulting in the simulated spectra shown in Fig. 2. The good agreement between the simulated and observed spectra suggests that the clusters shown in Fig. 1 represent the essential structural elements for the stoichiometric glasses. On the basis of our calculated results, we suggest an alternate assignment for the 250 cm^{-1} peak observed in Ge-rich compositions of $\text{Ge}_x\text{S}_{1-x}$.⁴ We attribute this feature to the ethanelike cluster shown in Fig. 2. The previous assignment⁴ of this peak was to a more Ge-rich structure with a nominal GeSe composition. We are currently investigating cluster models for this structure in order to establish its Raman signature in the near future.

This work was supported by the National Science Foundation (Grant No. DMR-RUI9972333) and by the Research Corporation. We thank Professor Punit Boolchand for many helpful discussions of the work prior to publication. We also thank Professor Shunji Sugai for permission to reproduce his data in Fig. 2.

¹G. Lucovsky, J. P. deNeufville, and F. L. Galeener, *Phys. Rev. B* **9**, 1591 (1974).

²G. Lucovsky, F. L. Galeener, R. C. Keezer, R. H. Geils, and H. A. Six, *Phys. Rev. B* **10**, 5134 (1974).

³S. Sugai, *Phys. Rev. B* **35**, 1345 (1987).

⁴P. Boolchand, J. Grothaus, M. Tenhover, M. A. Hazle, and R. K. Grasselli, *Phys. Rev. B* **33**, 5421 (1986).

⁵P. M. Bridenbaugh, G. P. Espinosa, J. E. Griffiths, J. C. Phillips, and J. P. Remeika, *Phys. Rev. B* **20**, 4140 (1979).

⁶R. J. Nemanich, S. A. Solin, and G. Lucovsky, *Solid State Com-*

mun. **21**, 273 (1977).

⁷Xingwei Feng, W. J. Bresser, and P. Boolchand, *Phys. Rev. Lett.* **78**, 4422 (1997).

⁸J. C. Phillips, *J. Non-Cryst. Solids* **34**, 153 (1979).

⁹M. F. Thorpe, *J. Non-Cryst. Solids* **57**, 355 (1983).

¹⁰G. Lucovsky, R. J. Nemanich, and F. L. Galeener, in *Proceedings of the 7th International Conference on Amorphous and Liquid Semiconductors, Edinburgh, Scotland, 1977*, edited by W. E. Spear (G. G. Stevenson, Dundee, Scotland, 1977), p. 130.

¹¹G. Lucovsky, C. K. Wong, and W. B. Pollard, *J. Non-Cryst.*

- Solids **59&60**, 839 (1983).
- ¹²K. Murase, T. Fukunaga, Y. Tanaka, K. Yajushiji, and I. Yunoki, *Physica B & C* **117B&118B**, 962 (1983).
- ¹³K. Inoue, O. Matsuda, and K. Murase, *J. Non-Cryst. Solids* **150**, 197 (1992).
- ¹⁴M. Cobb, D. A. Drabold, and R. L. Cappelletti, *Phys. Rev. B* **54**, 12 162 (1996).
- ¹⁵R. L. Cappelletti, M. Cobb, D. A. Drabold, and W. A. Kamitakahara, *Phys. Rev. B* **52**, 9133 (1995).
- ¹⁶C. Massobrio, A. Pasquarello, and R. Car, *Phys. Rev. Lett.* **80**, 2342 (1998).
- ¹⁷D. V. Porezag and M. R. Pederson, *Phys. Rev. B* **54**, 7830 (1996).
- ¹⁸P. Hohenberg and W. Kohn, *Phys. Rev.* **136**, B864 (1964).
- ¹⁹W. Kohn and L. J. Sham, *Phys. Rev.* **140**, A1133 (1965).
- ²⁰R. O. Jones and O. Gunnarson, *Rev. Mod. Phys.* **61**, 689 (1989).
- ²¹M. R. Pederson and K. A. Jackson, *Phys. Rev. B* **41**, 7453 (1990).
- ²²K. A. Jackson and M. R. Pederson, *Phys. Rev. B* **42**, 3276 (1990).
- ²³A. Briley, M. R. Pederson, K. A. Jackson, D. C. Patton, and D. V. Porezag, *Phys. Rev. B* **58**, 1786 (1998).
- ²⁴G. B. Bachelet, D. R. Hamann, and M. Schlüter, *Phys. Rev. B* **26**, 4199 (1982).
- ²⁵M. Cardona, in *Light Scattering in Solids II*, edited by M. Cardona and G. Güntherodt, Vol. 50 of *Topics in Applied Physics* (Springer, Berlin, 1982).
- ²⁶A. Komornicki and J. W. McIver, *J. Chem. Phys.* **70**, 2014 (1979).
- ²⁷K. Jackson and S. Grossman (unpublished).
- ²⁸P. Boolchand, J. Grothaus, W. J. Bresser, and P. Suranyi, *Phys. Rev. B* **25**, 2975 (1982).
- ²⁹H. C. Hsueh, M. C. Warren, H. Vass, G. J. Ackland, S. J. Clark, and J. Crain, *Phys. Rev. B* **53**, 14 806 (1996).
- ³⁰We calculate the binding energies of the clusters by first subtracting off the energy of the H-atom terminators and the X-H bonds on the cluster surfaces.